Preprint
UCRL-JC-149143

Laser Plasma Interactions with Intensities from 10^{12} W/cm^2 to 10^{21} W/cm^2

W.L. Kruer

This article was submitted to
44th Annual Meeting of the Division of Plasma Physics, Orlando, Florida, November 11-15, 2002

November 5, 2002

U.S. Department of Energy

Lawrence
Livermore
National
Laboratory

Laser plasma interactions with intensities from 10^{12} W/cm^2 to 10^{21} W/cm^2

William L. Kruer

Lawrence Livermore National Laboratory
P.O. Box 808 Livermore, California 94551

This invited paper was prepared
for the 44th annual meeting of the
APS Division of Plasma Physics

Work performed under auspices of the U.S. Department of Energy by the Lawrence Livermore National Laboratory under contract W-7405-Eng-48.

This work was performed under the auspices of the U.S. Department of Energy by the University of California, Lawrence Livermore National Laboratory under Contract No. W-7405-Eng-48.

Abstract

A tutorial introduction is given to some important physics and current challenges in laser plasma interactions. The topics are chosen to illustrate a few of John Dawson's many pioneering contributions to the physics and modeling of plasmas. In each case, a current frontier is also briefly discussed, including the .53μm option for laser fusion, kinetic inflation of instability levels, and new regimes accessed with ultra-high power lasers.

I. Introduction

A tutorial introduction is given to some important physics and current challenges in laser plasma interactions. All the topics addressed have a connection to various pioneering contributions of John M. Dawson to plasma physics and its applications during his Princeton years. His numerous seminal contributions to the physics and modeling of plasmas continue to have relevance and impact on the current frontiers.

Dawson was a visionary pioneer in basic plasma physics, computational physics, and in so many fields of plasma applications. These fields include fusion, laser plasmas, compact accelerators, isotope separation, space plasmas, and beam plasmas. Lasers were in their infancy (laser power of order gigawatts) when Dawson began to explore their use for fusion[1]. Likewise, computers were in their infancy (peak speed of order kiloflops) when he began to explore their use for modeling plasmas[2]. As shown in Figs. 1 and 2, his vision was on the mark. Since 1960, computers have increased in speed from kiloflops to many teraflops. Similarly, lasers have increased in focused intensity from about 10^{12} W/cm^2 to about 10^{21} W/cm^2.

Here some of Dawson's numerous contributions to laser plasmas are explored. Four different areas are considered: the high frequency resistivity of a plasma, its enhancement by ion density fluctuations, kinetic plasma effects, and ultra-intense laser plasma interactions. In each case, the discussion will touch upon an exciting current frontier, whether it be the .53μm options for laser fusion, the role of ion fluctuations in the saturation of stimulated Raman scattering, kinetic inflation of instability levels, or the new regimes being accessed with ultra-high power lasers.

II. Collisional absorption of laser light

Let's begin with the Dawson-Oberman calculation [3] of the high-frequency resistivity of a plasma, a key contribution to both basic plasma science and to many applications. In laser plasma applications, collisional absorption is typically the dominant absorption process. Indeed, the dependencies and scalings of the high frequency resistivity strongly impact the choice of laser wavelength and intensity for inertial confinement fusion.

In their elegant calculation, they considered a homogeneous pump field with frequency ω_0 and treated the ions as a set of randomly distributed point charges. Transforming to a frame oscillating with the electrons, they computed the average electric field which an ion feels due to the electrons and used this field to determine an impedance. The results are most simply described in terms of an effective collision frequency (ν_{eff}) for the energy dissipation of the pump field:

$$\nu_{eff} = \frac{\omega_{pe}^2}{\omega_0^2}\nu, \qquad \nu \approx \frac{Z\ln\Lambda}{11}\frac{\omega_{pe}}{N_D}. \tag{1}$$

Here ω_{pe} is the electron plasma frequency, Λ is a ratio of impact parameters, and N_D is the number of electrons in a Debye sphere. The dependencies of this collision frequency can be simply obtained by considering the deflection of an electron by an ion. For exact coefficients, see Ref 4.

For a plasma in thermal equilibrium, the resistivity is dominantly determined by high k fluctuations (i.e., by the very small scale length fluctuating microfields). However, when $\omega \approx \omega_{pe}$, there is a noticeable bump in the resistivity due to the excitation of electron plasma waves. This bump is shown in Figure 3, which is a plot of resistivity versus frequency. As we will discuss shortly, this bump can be greatly enhanced if ion fluctuations are excited to nonthermal levels.

Some simple estimates suffice to illustrate when collisional absorption is efficient. Consider laser light normally incident onto an isothermal plasma with density profile $n = n_{cr} \exp(-z/L)$, where n_{cr} is the critical density. The fractional absorption f_{abs} in this plasma is readily shown to be

$$f_{abs} = 1 - \exp(\frac{-8v^* L}{3c}), \qquad (2)$$

where v^* is the collision frequency evaluated at the critical density. To crudely estimate the electron temperature in the underdense plasma, we use a free-streaming model with a flux limit of .1, a value suggested by Fokker-Planck calculations of intense heat flow. In particular, $I_{abs} \cong .1 n_{cr} T_e v_e$ where I_{abs} is the absorbed intensity, T_e the electron temperature and v_e the electron thermal velocity. Combing these equations gives

$$f_{abs} = 1 - \exp(-\frac{I^*}{f_{abs} I}). \qquad (3)$$

Here $I^* = 10^{15}\, ZL/\lambda_\mu^4\ W/cm^2$ and L is in units of cm. Efficient absorption requires that $I \leq I^*$, a characteristic intensity which is a strong function of the laser light wavelength. Since $n_{cr} \propto \lambda_\mu^2$, shorter wavelength laser light penetrates denser and cooler plasma, which is much more collisional.

From the standpoint of collisional absorption, note that .53 μm light is acceptable for laser fusion applications. If we consider an example from direct drive (Z=3 and L=.1cm), $I^* \sim 5x10^{15}\, W/cm^2$ for .53μm light. Thus the absorption is quite efficient for intensities of 1-2x10^{15} W/cm^2 which are typically used. Of course, collisional absorption is even more efficient for indirect drive targets, which include regions of high Z plasma.

Using the National Ignition Facility to also output frequency-doubled (.53 μm) light is an exciting possibility which is being very actively explored. As discussed by E. M. Campbell *et. al.*[5], this option is especially attractive, since the higher glass damage thresholds for .53μm light would enable significantly more laser energy to be output. In addition, significantly more bandwidth (>2 times) can be obtained, enabling more beam smoothing. Theoretical scalings suggest that laser plasma instabilities will have comparable levels to those obtained with .35μm light, provided the laser intensity is reduced about a factor of two. Recent interaction physics experiments using .53μm light at both LLE[6] and at AWE[7] look promising. Stimulated scattering levels are about the same as in comparable experiments with .35μm light. Moreover, recent target designs by L. Suter[8] show that the additional energy allows new options for design of larger targets for which the peak laser intensity is significantly lower than that used in the mainline designs for .35μm light. More interaction physics experiments using .53μm light with even longer scalelength plasmas are now being planned to further explore this exciting option to enhance the capabilities of NIF.

III. Enhancement of the high-frequency resistivity by ion density fluctuations

Dawson and Oberman went on to show that the high-frequency resistivity could be significantly enhanced[9] by a nonthermal level of ion density fluctuations.A very simple treatment of this important effect can be given. Consider a plasma with a spectrum of density fluctuations which we approximate as static:i.e., $n = n_o + \sum_k \delta n_k \cos k \bullet x$. Again treat the high frequency wave as a homogeneous pump field with amplitude $E = E_0 \cos(\omega_0 t)$. By oscillating electrons in the presence of the density fluctuations, the pump field creates high frequency density fluctuations and their corresponding self-consistent electric fields. The damping of the pump field is determined by balancing its rate of energy loss with the rate of energy dissipated by the driven plasma fields. It is readily shown that the effective collision frequency for the pump field becomes[10]

$$\nu_{eff} = \frac{\omega_0}{2} \sum \left(\frac{\delta n_k}{n_{cr}} \right)^2 \mathrm{Im} \frac{1}{\varepsilon_L(k,\omega_0)} \cos^2 \theta_k \, , \qquad (4)$$

where θ_k is the angle between k and E_0, n_{cr} is the critical density at which $\omega_{pe} = \omega_0$, and $\varepsilon_L(k,\omega)$ is the usual plasma dispersion function.

This damping can readily exceed the collisional damping. For example, let's consider a density fluctuation with amplitude $\delta n = .1 n_{cr}$ and with a wave number $k\lambda_{De} = .5$ aligned along the electric vector. Then $\nu_{eff} \sim 5x10^{-3}\omega_0$ for either an electron plasma wave or for a light wave near its cutoff density. Indeed, an enhanced absorption of laser light propagating through a rather underdense plasma has recently been reported[11]. This anomalous absorption was attributed to an enhanced resistivity due to sound waves excited by a return current instability.

There are a variety of mechanisms to produce enhanced density fluctuations. These fluctuations can be generated by laser-driven plasma instabilities. A high frequency pump field beats with a thermal level density fluctuation to generate a high frequency wave. This in turn beats with the pump field to produce a fluctuation in the electric field pressure which generates a density fluctuation. With frequency and wave number matching, this feedback leads to growth of the density fluctuations. Examples of this resonant coupling are the Langmuir wave decay instability (an electron plasma wave decays into another electron plasma wave plus an ion sound wave) and the stimulated Brillouin instability (a light wave decays into another light wave plus an ion sound wave). Other sources for these density fluctuations include intensity structure in the laser beam[12] (either existing or due to filamentation), differential plasma expansion, and a return current instability driven by intense heat flow, already mentioned above.

Long wavelength ion density fluctuations can be especially important for electron plasma waves due to quasi-resonant mode coupling[13], as discussed by Kaw, Lin and Dawson. Consider a very long wavelength electron plasma wave with amplitude E_0 and frequency ω_0 in a cold plasma which includes a static density fluctuation with amplitude δn and wave number k.. The plasma wave mode couples with the density fluctuation to produce another high frequency wave with $E(k,\omega_0)$:

$$E(k,\omega) = \frac{E_0}{\varepsilon_L(k,\omega)} \frac{\delta n}{n_{cr}}. \qquad (5)$$

When $\delta n/n_{cr} \geq |\varepsilon_L(k,\omega_0)|$, $E(k,\omega_0)$ becomes comparable to E_0 . This field in turns mode couples with the density fluctuation to produce $E(2k,\omega_0)$. This repeated mode coupling continues until $|\varepsilon_L(Nk,\omega_0)|$ significantly exceeds $\delta n/n_{cr}$, generating a series of shorter wavelength high frequency waves. Consequences[14] include an enhanced damping of the primary wave and a reduction in the energy of the heated electrons. This quasi-resonant mode coupling has been observed in detail in laser beat-wave experiments[15].

Recent simulations [16] of strongly-driven stimulated Raman scattering in a plasma with near .25 n_{cr} demonstrate the self-consistent generation of long wavelength ion density fluctuations and some dramatic consequences. Consider a one-dimensional PIC simulation of .53μm laser light with intensity of 7×10^{15} W/cm^2 propagating through an initially uniform plasma with a density of .23 n_{cr}. As shown in Fig. 4, the plasma density in the nonlinear state becomes very strongly rippled with long wavelength density fluctuations. These fluctuations have a wavelength about three times the wavelength of the laser light and are self-consistently driven by stimulated Brillouin scattering of the Raman-scattered light wave, which is near its critical density. These strong fluctuations reduced the effective temperature of the heated electron to about 25 keV, in agreement with measurements[8] using the Helen laser at AWE.

IV. Kinetic plasma effects

John was a pioneer in the understanding and modeling of kinetic plasma effects. He gave a very physical treatment of Landau damping, which greatly clarified this fundamental process. By calculating the energy changes for particles moving in a wave, he showed[17] that a damping of the wave resulted if more particles were going slower than the phase velocity of the wave than were going faster. By averaging the energy changes over a distribution of velocities, he reproduced the Landau damping coefficient obtained from the Vlasov equation. He also showed that an electron plasma wave would break[18] when its amplitude reached a critical value. In a cold plasma this wavebreaking occurs when the oscillation velocity of electrons becomes equal to the phase velocity ($eE/m\omega_{pe} = v_p$). At wave breaking very strong electron heating of electrons onsets. In general, nonlinear kinetic effects are very difficult to describe analytically. Hence Dawson turned to computer simulation of plasmas using particles[2,19], which has proved to be a very powerful and widely used tool for modeling nonlinear kinetic plasma phenomena. Particle codes now commonly solve relativistic equations of motion and the complete set of Maxwell's equations. In a recent three-dimensional simulation by Bert Still[20], approximately 7 billion particles were used.

Kinetic plasma effects have been very important in laser plasmas. There's often an anomalous heating of plasmas by intense laser light due to the excitation of plasma waves via a variety of instabilities (and also by mode conversion). In general, this heating results in the formation of high energy tails on the distribution functions. An early example[21] of this tail formation on both the electron and ion distribution functions is shown in Fig. 5. In this simulation, the electron plasma waves and ion acoustic waves were driven unstable by an pump field with frequency near the electron plasma frequency. Such suprathermal tail formation is particularly important for laser fusion, since high energy electrons can preheat the fuel and prevent the large compressions needed for high gain.

An exciting current issue is to better understand the role of kinetic effects on the saturation of stimulated Raman and Brillouin scattering in long scalelength plasmas. Instability thresholds and gains commonly depend explicitly on the Landau damping rate, which in turn greatly varies as the distribution function nonlinearly distorts. For example, let's consider stimulated Brillouin scattering[22] (SBS) on heavily damped ion waves, a regime very relevant to gas-filled hohlraum targets. The instability gain then varies inversely with the Landau damping rate for the ion acoustic waves. However, the linear damping coefficient is only valid for a time $<< \omega_{bi}^{-1}$, where ω_{bi} is the bounce frequency of an ion in the potential trough of the ion sound wave. Even for a small amplitude ion wave this time is quite short. For example, for a wave amplitude of $\delta n/n = .01$ and typical plasma parameters appropriate to an ignition target, t<1ps. On a longer time scale, the slope of the distribution function flattens[23], and the Landau damping goes away, leading to an enhancement of the SBS. This effect has also been demonstrated by Vu et. al. in simulations[24] of stimulated Raman scattering, where the enhanced SRS is described as kinetic inflation.

In the simulations of SBS, it was shown that sometimes ion-ion collisions can maintain the slope of the distribution function and hence the Landau damping. Fig. 6a shows the temporal evolution of the velocity perturbation associated with an initially-excited ion sound wave, with and without ion-ion collisions. In this example, the plasma is an equal mixture of Au^{+50} and Be^{+4} with an electron temperature of 3 keV, an ion temperature of 1.5 keV, an electron plasma density of .25 n_{cr} for .35μm light. The ion wave has a wave number twice that of a .35μm light wave. Initially the wave Landau damps at the predicted rate. Without collisions, the damping ceases at $t \sim \pi/\omega_{bi}$. With collisions the slope is preserved, and the damping continues until the amplitude is quite small. A snapshot of the distribution function in Fig. 6b shows the distribution function distorting in one case but remaining nearly Maxwellian in the other. In the corresponding simulation in which the plasma was irradiated with a .35μm light wave with intensity $2x10^{15}$ W/cm^2, the reflectivity due to SBS was small (~1%) with ion collisions, but became quite significant (~30%) without collisions. Similar results were found for CH plasmas.

V. Ultra-intense laser plasma interactions

The most exciting and dynamic new frontier is ultra-intense laser matter interactions. This new frontier was opened up by the development of ultrashort and ultrahigh power lasers using chirped pulse amplification[25]. Such lasers typically have pulse lengths of order 100 fs to 1 ps and have now been focussed to intensities up to about 10^{21} W/cm2. The first petawatt laser was achieved in 1997 using a beam line of the Nova laser at LLNL. There are currently petawatt lasers in operation in Japan and the UK, with others in the planning stage in the US and elsewhere.

For very high intensities the light pressure is extremely large. In particular,

$$\frac{I}{c} \cong 330 \frac{I}{10^{18}} Mbar, \tag{6}$$

where I is the intensity in W/cm^2. Likewise, the electron dynamics become strongly relativistic; i.e.,

$$\left(\frac{p_{os}}{m_o c}\right)^2 \cong \frac{I \lambda_\mu^2}{1.35x10^{18}}, \tag{7}$$

where p_{os} is the momentum of oscillation in the transverse electric field and m_0 is the electron rest mass.

Characteristically, Dawson was already envisioning such high intensities over 30 years ago. Kaw and Dawson[26] analyzed an effect which can be described as induced transparency. For simplicity, consider a cold plasma and a circularly polarized light wave with vector potential $A = A_0\left[\bar{x}\cos(kx - \omega t) + \bar{y}\sin(kz - \omega t)\right]$. Note that p_z=0 and also that $|p_t|^2$ and γ are then independent of time, where p_z (p_t) is the longitudinal (transverse) momentum of an electron in the light wave. Substituting $B = \nabla x A$ into Faraday's law, one readily obtains the wave equation for the light wave

$$\left(\frac{\partial^2}{\partial t^2} - c^2\nabla^2\right)A = -\frac{\omega_{pe}^2 A}{\sqrt{1+\left(\frac{eA}{m_0 c^2}\right)^2}}. \tag{8}$$

The dispersion relation becomes

$$\omega^2 = k^2c^2 + \frac{\omega_{pe}^2}{\sqrt{1+(\frac{eA_0}{m_0c^2})^2}} . \tag{9}$$

It is apparent that the maximum plasma density for light wave propagation is increased. The relativistic mass correction lowers the effective plasma frequency, enabling propagation in what would otherwise be an overdense plasma. Referring to Eq. 1, this induced transparency requires laser intensities of order $I\lambda_\mu^2 \geq 10^{18}\,W - \mu^2/cm^2$ in order to be significant, which was of course beyond then the state of the art .

Laser experiments with such intensities are now common, and PIC codes are proving to be very powerful tools to investigate the strongly nonlinear, relativistic kinetic phenomena. The simulations have illustrated many key features of this relativistic plasma regime. These include multi-meV electron and ion generation, hole boring, very high harmonic generation, and self-generated magnetic fields as large as 10^9 Gauss. Applications under active investigation range from new diagnostic sources to fast ignition.

Let's consider several exciting recent advances. Extremely large self-generated magnetic fields have now been observed. Very impressive magnetic fields around the laser spot were found in early computer simulations[27] using normally-incident ultra-intense light. As a rule of thumb, B_{dc}~$B_{os}/3$, where B_{dc} (B_{os}) is the self-generated (oscillating laser) magnetic field. This corresponds to a field of 10^8 Gauss for 1.06μm light with I=10^{18} W/cm^2 and 10^9 Gauss for I=10^{21} W/cm^2. Recently Tatarakis *et. al.*[28] measured the self-generated fields around the heated spot using polarimetry of various harmonics of the light wave. In these experiments .7-1ps pulses of 1.06μm light was obliquely incident onto planar targets, and the laser intensity was varied from 10^{18}-10^{20} W/cm^2. Fig 7 shows the values inferred versus laser intensity. A self-generated field as high as 4x10^8 Gauss was measured at I~10^{20} W/cm^2. Detailed PIC simulations using obliquely-incident light were in good agreement with the observations.

As a second example, high quality proton beams have been produced in experiments[29] with ultra-intense laser irradiation. These ions are accelerated to high energy in the MeV/μm sheath electric fields produced by the relativistic electrons at the target-vacuum interface at the rear of the target. (High energy ions are also directly generated at the light plasma interface by the enormous radiation pressure.) Recent simulations by Wilks et. al[30]. show that the energetic ions from the rear surface can be focused by using a suitably curved target., an effect now being search for in experiments. The high energy proton beams have been successfully used[31] to directly probe the electric fields in dense plasmas. Many other applications are being considered, including a possible use for fast ignition.

VI. Summary

In this tutorial introduction, four significant areas of laser plasma physics have been considered in order to illustrate a few of John Dawson's many pioneering contributions to plasma science and modeling. His work clearly has had great impact and continues to be very relevant to exciting current frontiers. In addition to his wide-ranging contributions in so many different areas of plasma physics, he was an extremely caring teacher and mentor to many, many young scientists. He was very generous with his time and ideas, and his enthusiasm for science was truly contagious. What a remarkable legacy he has left!

Acknowlegments: This paper is based on an invited talk in the Dawson Memorial Session at the 44th annual meeting of the APS Division of Plasma Physics. I am grateful to numerous colleagues for valuable discussions and interactions, especially with Scott Wilks, Warren Mori, Dan Gordon, Larry Suter, John Moody, Peter Rambo, Michael Ortelli, David Jones, and Marty Wallace. I also gratefully acknowledge the colleagues who have generously allowed me to use figures from their recent work., as noted in the paper.
This work was performed under the auspices of the U. S. Department of Energy by the Lawrence Livermore National laboratory under Contract W-7405-Eng-48.

References

1. John M. Dawson, Phys. Fluids 7, 981 (1964)
2. John M. Dawson, Phys. Fluids 5, 455 (1962)
3. John Dawson and Carl Oberman, Phys. Fluids 5, 517 (1962)
4. T. W. Johnston and J. M. Dawson, Phys. Fluids 16, 772 (1973)
5. E. M. Campbell, D. Eimerl, W. L. Kruer, S. Weber, and C. P. Verdon, Comments Plasma Phys. Controlled Fusion 18, 201 (1997)
6. John Moody *et. al.*, Bull. Am. Phys. Soc. (2002)
7. Kevin Oades *et. al.*, Bull. Am. Phys. Soc. 46, 292 (2001)
8. L. Suter, Bull. Am. Phys. Soc. 46, 296 (2001)

9. John Dawson and Carl Oberman, Phys. Fluids 6, 394 (1963)
10. R. J. Faehl and W. L. Kruer, Phys. Fluids 20, 55 (1977)
11. S. H. Glenzer *et. al.*, Phys. Rev. Lett. 88, 235002 (2002)
12. John Moody *et. al.*,., Phys. Rev. Lett. 83, 1783 (1999)
13. P. K. Kaw, A. T. Lin, and J. M. Dawson, Phys. Fluids 16, 1967 (1973)
14. W. L. Kruer, Phys. Fluids 15, 2423 (1972)
15. C. Darrow *et .al.*, Prys. Rev. Lett. 56, 2629 (1986)
16. D. Jones, M. Ortelli, M. Wallace, *et. al.* , to be published
17. J. M. Dawson, Phys. Fluids 4, 869 (1961)
18. J. M. Dawson, Phys. Rev. 113, 383 (1959)
19. J. M. Dawson Phys. Fluids 5, 445 (1962); J. M. Dawson, Rev. of Mod. Phys. 55, 403 (1983)
20. Bert Still, private communication
21. W. L. Kruer, P. K. Kaw, J. M. Dawson, and Carl Oberman Phys. Rev. Lett. 24, 987 (1969)
22. P. W. Rambo, S. C. Wilks, and W. L. Kruer, Phys. Rev. Lett. 79, 83 (1997); William L. Kruer, Bedros B. Afeyan, A. E. Chou, R. K. Kirkwood, D. S. Montgomery, P. W. Rambo, and S. C. Wilks, Physica Scripta T75, 7 (1998)
23. T. M. O'Neil, Phys. Fluids 8, 2255 (1965)
24. H. X. Vu, D. F. DuBois, and B. Bezzerides, Phys. Rev. Lett. 86, 4306 (2001); X. Vu, D. F. DuBois, and B. Bezzerides, Phys. Plasmas 9, 1 (2002)
25. M. D. Perry and G. Mourou, Science 264, 917 (1994)
26. P. K. Kaw and J. M. Dawson, Phys. Fluids 13, 472 (1970)
27. S. C. Wilks, W. L. Kruer, A. B. Langdon, and M. Tabak, Phys. Rev. Lett. 74, 25 (1995)
28. M. Tatarakis, *et. al.*, Phys. Plasmas 9, 2244 (2002)
29. M. Key *et. al.*, in Proceedings of the 17th IAEA Fusion Energy Conference (International Atomic Energy Agency, Vienna, 1999), Vol. 3, p. 1093;
30. S. C. Wilks, A. B. Langdon, T.E. Cowan, M. Roth, M. Singh, S. Hatchett, M. H. Key, D. Pennington, A. MacKinnon, and R. A. Snavely, Phys. Plasmas 8, 542 (2001)
31. M. Borghesi, *et. al.*, Phys. Plasmas 9, 2214 (2002)

Figure captions

Fig. 1: The evolution of computer power as illustrated by the succession of computers at the Lawrence Livermore National laboratory.

Fig. 2: The evolution of the laser intensity since 1960 (compliments G. Mourou).

Fig. 3: A plot of the high frequency resistivity of a plasma versus frequency (from ref. 3).

Fig. 4: A snapshot of the plasma density in a PIC simulation of intense laser light propagating through a plasma with initial density of .23 n_{cr} (from ref. 16).

Fig. 5: The electron and ion velocity distribution functions from a PIC simulation of a plasma driven by a pump field oscillating near ω_{pe} (from ref. 21).

Fig. 6: a) the time history of the velocity perturbation associated with an initially-excited ion sound wave and b) the velocity distribution of the Be ions in the nonlinear state (from ref. 22).

Fig. 7: Measurements of the self-generated magnetic field around the laser spot as determined by polarimetry of the harmonics (from ref. 28).

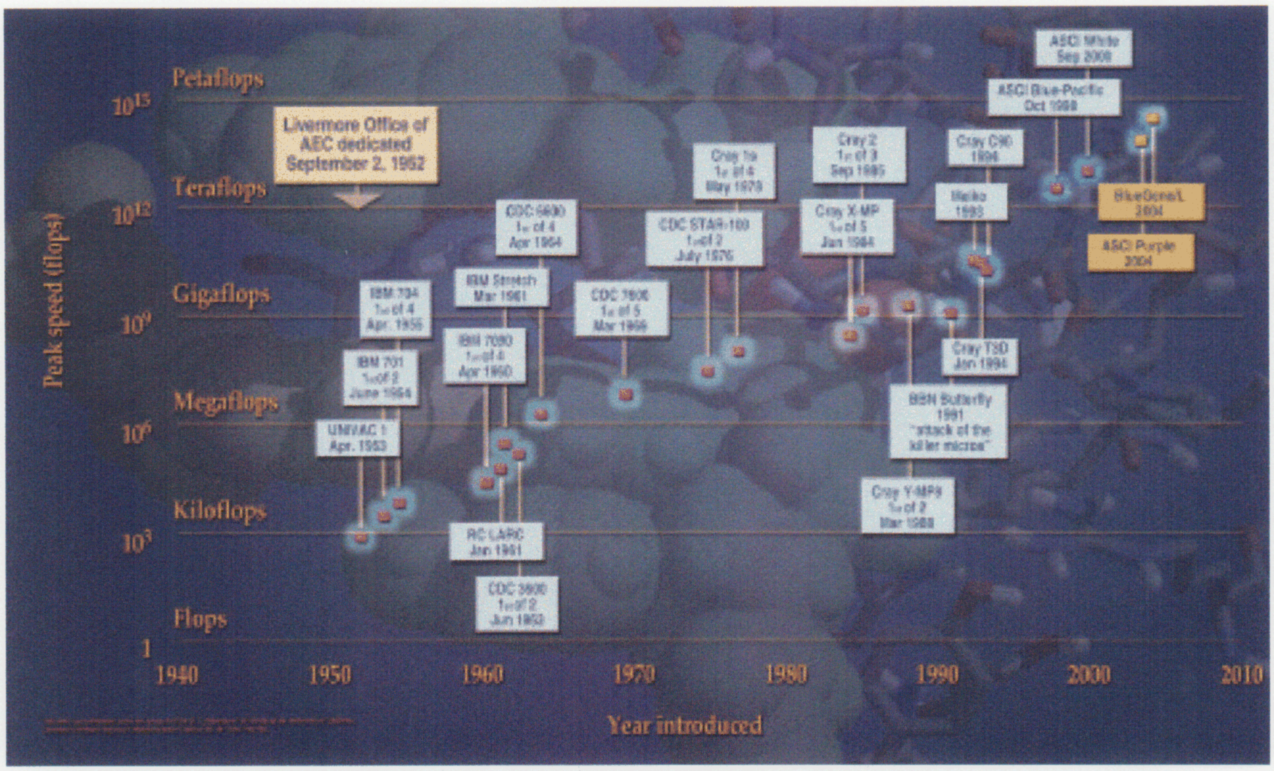

Petaflops
Teraflops
Gigaflops
Megaflops
Kiloflops
Flops
Peak speed (flops)
Year introduced
Livermore Office of AEC dedicated September 2, 1952
UNIVAC 1 Apr. 1953
IBM 701 1st of 2 June 1954
IBM 704 1st of 4 Apr. 1955
IBM 7090 1st of 4 Apr 1960
IBM Stretch Mar 1961
RC LARC Jan 1961
CDC 3600 1st of 2 Jun 1963
CDC 6600 1st of 4 Apr 1964
CDC 7600 1st of 5 Mar 1969
CDC STAR-100 1st of 2 July 1976
Cray 1s 1st of 4 May 1979
Cray X-MP 1st of 5 Jan 1984
Cray 2 1st of 3 Sep 1985
Cray Y-MP8 1st of 2 Mar 1988
BBN Butterfly 1991 "attack of the killer micros"
Cray T3D Jan 1994
Meiko 1993
Cray C90 1994
ASCI Blue-Pacific Oct 1998
ASCI White Sep 2000
BlueGene/L 2004
ASCI Purple 2004

FIG 1

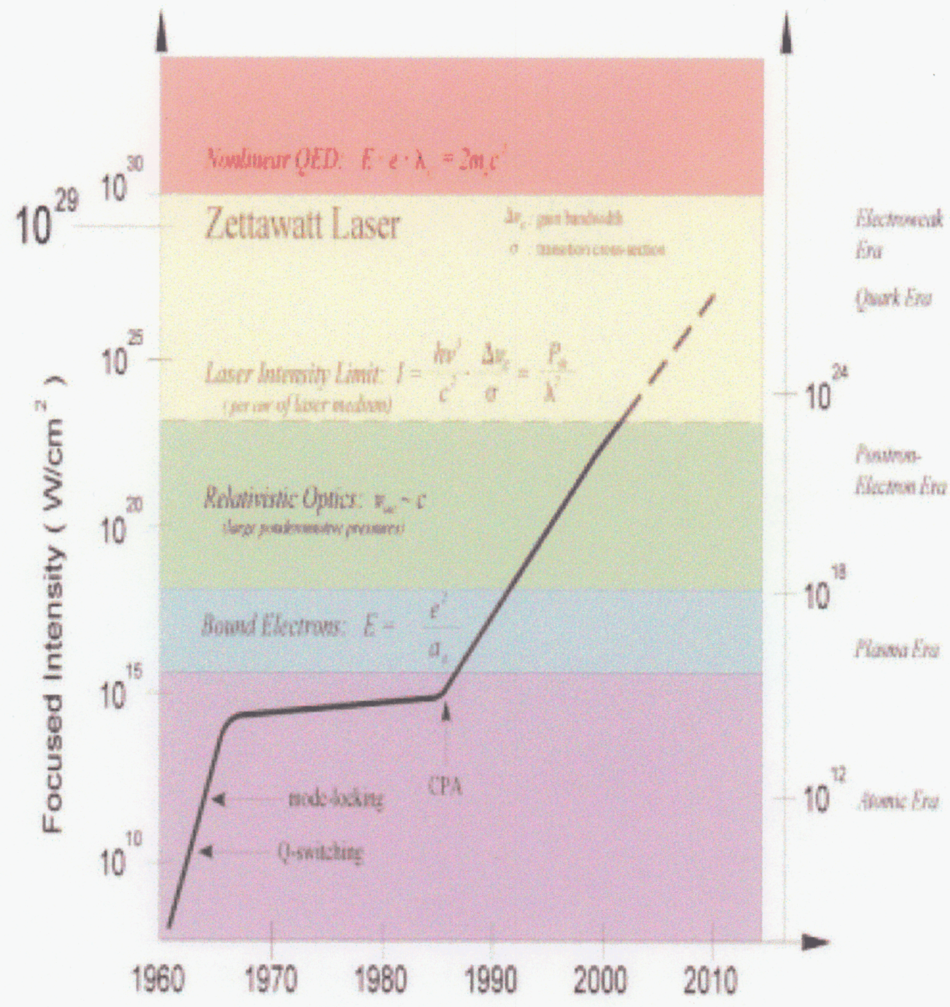

Nonlinear QED: $E \cdot e \cdot \lambda_c = 2m_e c^2$
Zettawatt Laser
Laser Intensity Limit: $I = \frac{h\nu^3}{c^2} \cdot \frac{\Delta\nu_g}{\sigma} = \frac{P_{th}}{\lambda^2}$
(per cm² of laser medium)
Relativistic Optics: $v_{osc} \sim c$
(large ponderomotive pressures)
Bound Electrons: $E = \frac{e^2}{a_0}$
mode-locking
Q-switching
CPA
Focused Intensity (W/cm^2)
10^{29}
10^{30}
10^{25}
10^{20}
10^{15}
10^{10}
10^{24}
10^{18}
10^{12}
Electroweak Era
Quark Era
Positron-Electron Era
Plasma Era
Atomic Era
1960
1970
1980
1990
2000
2010

FIG 2

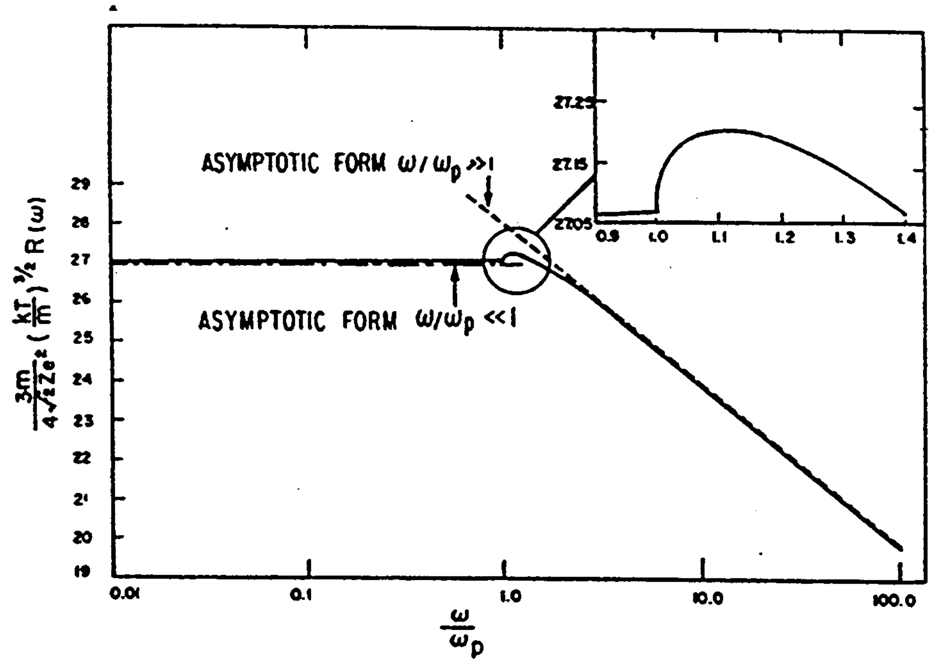

ASYMPTOTIC FORM $\omega/\omega_p \gg 1$
ASYMPTOTIC FORM $\omega/\omega_p \ll 1$
$\frac{3m}{4\sqrt{2}Ze^2}\left(\frac{kT}{m}\right)^{3/2} R(\omega)$
$\frac{\omega}{\omega_p}$
0.01
0.1
1.0
10.0
100.0
19
20
21
22
23
24
25
26
27
28
29
27.25
27.15
27.05
0.9
1.0
1.1
1.2
1.3
1.4

FIG 3

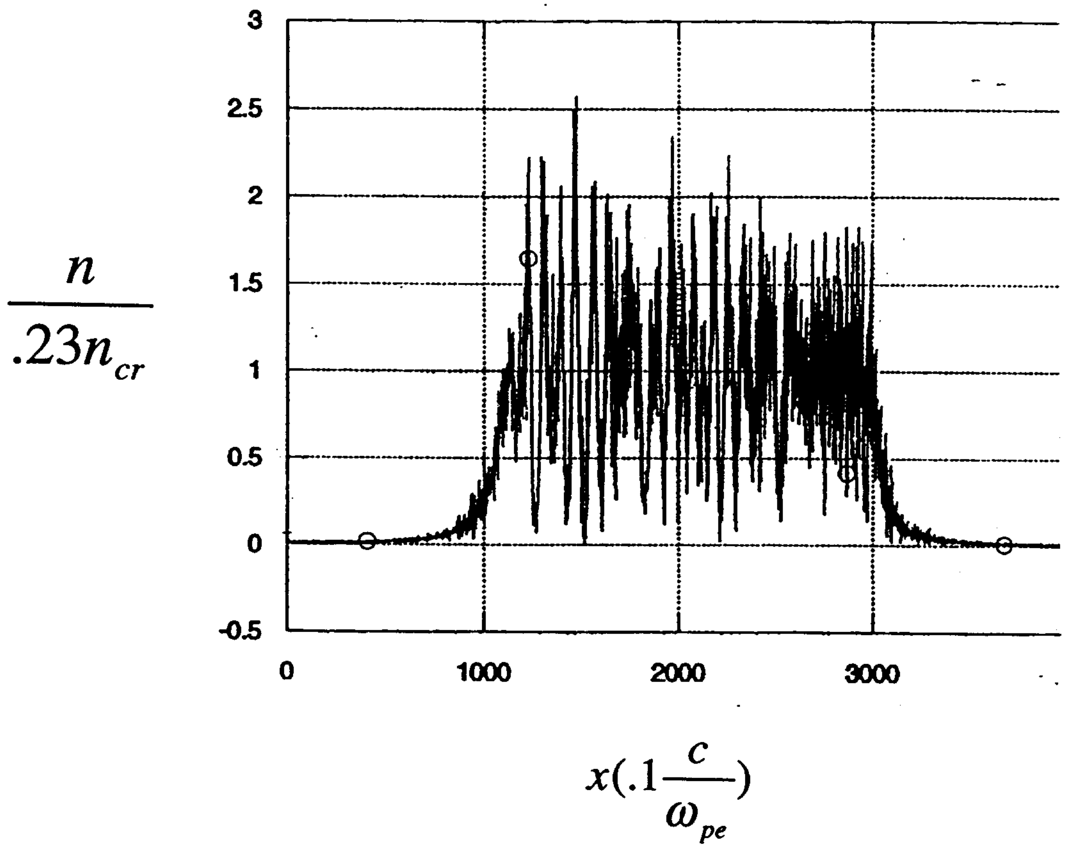

FIG 4

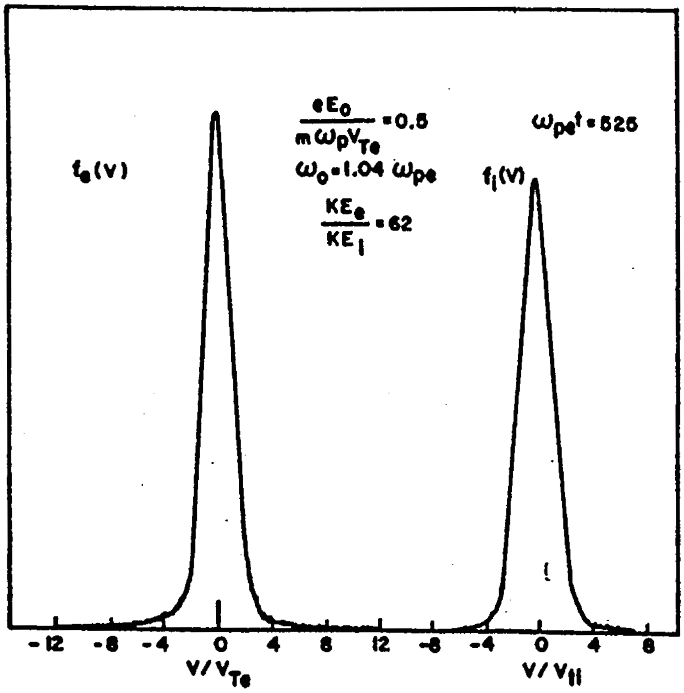
$\frac{eE_0}{m\omega_p v_{Te}} = 0.5$
$\omega_0 = 1.04\ \omega_{pe}$
$\frac{KE_e}{KE_i} = 62$
$\omega_{pe}t = 525$
$f_e(v)$
$f_i(v)$
-12 -8 -4 0 4 8 12 -8 -4 0 4 8
v/v_{Te}
v/v_{ti}

Fig 5

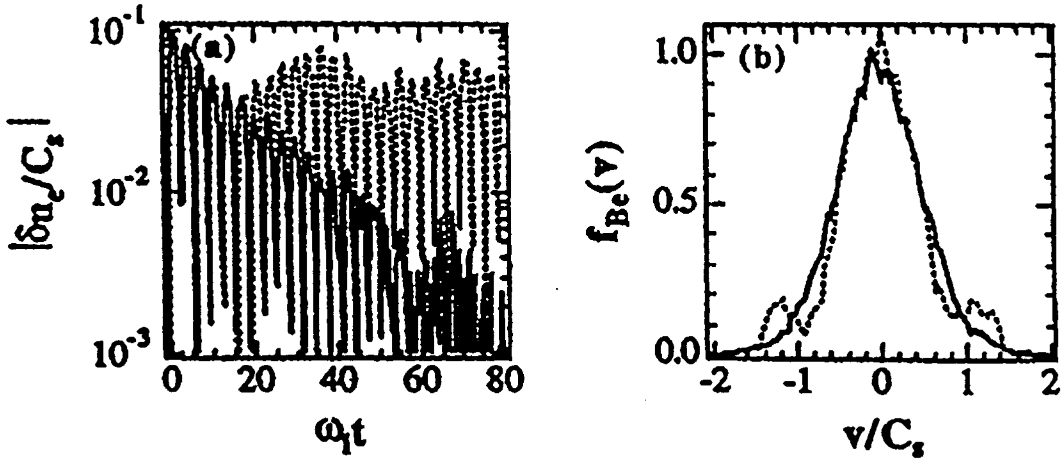

(a)
10^{-1}
10^{-2}
10^{-3}
$|\delta n_e/C_s|$
0
20
40
60
80
$\omega_i t$
(b)
1.0
0.5
0.0
$f_{Be}(v)$
-2
-1
0
1
2
v/C_s

FIG 6

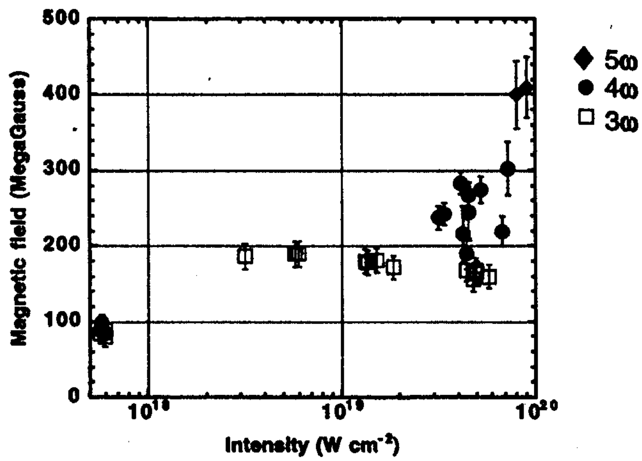

500
400
300
200
100
0
Magnetic field (MegaGauss)
Intensity (W cm⁻²)
5ω
4ω
3ω

FIG 7